

Remodeling of Substance P Sensory Nerves and Transient Receptor Potential Melastatin 8 (TRPM8) Cold Receptors After Corneal Experimental Surgery

Jiucheng He,^{1,2} Thang Luong Pham,¹ Azucena H. Kakazu,¹ and Haydee E. P. Bazan^{1,2}

¹Neuroscience Center of Excellence, School of Medicine, Louisiana State University Health New Orleans, New Orleans, Louisiana, United States

²Department of Ophthalmology, School of Medicine, Louisiana State University Health New Orleans, New Orleans, Louisiana, United States

Correspondence: Haydee E. P. Bazan, Neuroscience Center of Excellence and Department of Ophthalmology, School of Medicine, Louisiana State University Health, New Orleans, LA 70112, USA; hbazan1@lsuhsc.edu.

Submitted: December 7, 2018

Accepted: April 29, 2019

Citation: He J, Pham TL, Kakazu AH, Bazan HEP. Remodeling of substance P sensory nerves and transient receptor potential melastatin 8 (TRPM8) cold receptors after corneal experimental surgery. *Invest Ophthalmol Vis Sci*. 2019;60:2449-2460. <https://doi.org/10.1167/iovs.18-26384>

PURPOSE. To investigate changes in corneal nerves positive to substance P (SP) and transient receptor potential melastatin 8 (TRPM8) and gene expression in the trigeminal ganglia (TG) following corneal surgery to unveil peripheral nerve mechanism of induced dry eye-like pain (DELP).

METHODS. Surgery was performed on mice by removing the central epithelial and anterior stromal nerves. Mice were euthanized at different times up to 15 weeks. Immunostaining was performed with TRPM8, SP, or protein gene product 9.5 (PGP9.5) antibodies, and epithelial nerve densities were calculated. The origin of TRPM8- and SP-TG neurons were analyzed by retrograde tracing. Gene expression in TG was studied by real-time PCR analysis.

RESULTS. SP-positive epithelial corneal nerves were more abundant than TRPM8 and were expressed in different TG neurons. After injury, epithelial nerve regeneration occurs in two distinct stages. An early regeneration of the remaining epithelial bundles reached the highest density on day 3 and then rapidly degraded. From day 5, the epithelial nerves originated from the underlying stromal nerves were still lower than normal levels by week 15. The SP- and TRPM8-positive nerve fibers followed the same pattern as the total nerves. TRPM8-positive terminals increased slowly and reached only half of normal values by 3 months. Corneal sensitivity gradually increased and reached normal values on day 12. Corneal injury also induced significant changes in TG gene expression, decreasing *trpm8* and *tac1* genes.

CONCLUSIONS. Abnormal SP expression, low amounts of TRPM8 terminals, and hypersensitive nerve response occur long after the injury and changes in gene expression in the TG suggest a contribution to the pathogenesis of corneal surgery-induced DELP.

Keywords: corneal innervation, TRPM8, SP, neuropathic pain, refractive surgery

The cornea, mainly innervated by sensory nerves originated from neurons in the ophthalmic division of trigeminal ganglia (TG), is a powerful pain generator in the human body. The density of corneal pain receptors has been estimated to be 40 times that of the dental pulp.¹ Diseases and ophthalmic surgical procedures that damage corneal nerves can induce dry eye and corneal neuropathic pain, also called dry eye-like pain (DELP).² Photorefractive keratectomy (PRK) and laser-assisted in situ keratomileusis (LASIK), two of the most common procedures performed to correct vision, are well-known inducers of DELP.³⁻⁷ In PRK, the removal of the epithelium injures the epithelial nerve terminals, and in LASIK procedures, epithelial nerve bundles and superficial stromal nerve branches in the flap interface are cut by a microkeratome. Additional damage to the stromal nerves is caused by excimer laser photo ablation. It has been reported that 60% of LASIK patients experience DELP 1 month after the surgery, and 50% of these patients still have symptoms of ocular dryness and irritation after 6 months.⁶⁻¹³ In some cases, extensive DELP symptoms may persist for years, regardless of no apparent clinical signs of dry eye.^{7,14-16}

Corneal sensory nerves are functionally heterogeneous. Electrophysiologic experiments have classified the nerves fibers as polymodal nociceptors, mechanical nociceptors, and cold-sensitive receptors.¹⁷ Damage caused by corneal nerve injury disrupts transmission of these receptors to the TG and to the thalamus and somatosensory cortex, causing sensations of discomfort or pain.^{2,16} DELP involves both nociceptive and neuropathic symptoms. Recent studies have reported that PRK surgery and aging give rise to both functional and morphologic alterations in mechanical, polymodal, and cold sensory nerve fibers of the cornea, suggesting the involvement of neuropathic mechanism in DELP.^{18,19}

Neuropeptides released from trigeminal fibers fulfill well-known functions in neuroinflammatory processes and in the modulation of nociceptive signal processing. Substance P (SP) has a wide range of effects, including nociception (pain perception) and neurogenic inflammation.^{20,21} Recent studies from our lab have shown that, in mouse cornea, SP-positive nerves take up about 59% of total epithelial innervation and that there is a significant decrease of SP nerves in diabetic mice.^{22,23} Transient receptor potential melastatin (TRPM8) is an

ion channel expressed in sensory neurons that play an important role as a cold sensor and respond to changes in osmolarity.^{24,25} Studies have shown that TRPM8 regulates the wetting of the ocular surface and that altered expression of the TRPM8 channel contributed to cold allodynia and neuropathic pain.^{26–30} There are changes in morphology and function of TRPM8 axons and terminals in aging mice. These changes are associated with an increase in tearing, characteristic of dry eye in older people.¹⁹ A clinical study also reported that subjects with dry eye disease had greater sensitivity to cold than normal subjects and found that DELP duration was critical to cooling sensitivity.³¹

In the current study, we used a mouse wound model that mimics refractive surgery to investigate the changes in epithelial nerve regeneration, SP- and TRPM8-labeled sensory nerves, and terminals, as a function of time after corneal injury. Functional assays of corneal sensitivity and tear secretion were also investigated. To analyze the response in the TG after corneal damage of the sensory nerves and terminals, gene expression of SP and TRPM8, as well as genes involved in inflammation and repair were followed at different times after corneal injury.

MATERIALS AND METHODS

Animals

Adult Swiss Webster mice of both sexes, aged 8 to 10 weeks were purchased from Charles River Laboratories (Wilmington, MA, USA) and housed at the Neuroscience Center of Excellence Animal Care, Louisiana State University Health (LSUH; New Orleans, LA, USA). The animals were handled in compliance with the guidelines of the ARVO Statement for the Use of Animals in Ophthalmic and Vision Research, and the experimental protocol was approved by the Institutional Animal Care and Use Committee at LSUH.

Antibodies

Rabbit monoclonal anti-protein gene product 9.5 (PGP9.5, EPR4118) and rabbit monoclonal anti-TRPM8 (EPR4196) antibodies were purchased from Abcam Inc. (Cambridge, MA, USA). Rat monoclonal (NC1/34HL) anti-SP was purchased from Santa Cruz Biotechnology (Dallas, TX, USA). Secondary antibodies Alexa fluor 488 goat anti-rabbit IgG (H+L), anti-rat IgG (H+L), Alexa fluor 594 goat anti-rat IgG (H+L), and Alexa Cy5 goat anti-rabbit were purchased from Invitrogen (Carlsbad, CA, USA).

In Vivo Corneal Injury Model

Mice were anesthetized by intraperitoneal injection of ketamine (200 mg/kg) and xylazine (10 mg/kg). After topical application of one drop of proparacaine-HCl 0.5%, the right eye was injured by removing the epithelium and one-third of the anterior stroma of a 2-mm-diameter central area by using a corneal rust ring remover, as previously described.²² After injury, the eyes received 0.3% tobramycin eyedrops (Henry Schein, Melville, NY, USA) three times daily for 3 days to prevent infection.

Corneal Sensitivity

Corneal sensitivity within the central area (about 2 mm in diameter) was measured in nonanesthetized mice under a surgical loupe with a Cochet-Bonnet esthesiometer, as previously described.^{22,32} Briefly, the length of the monofilament was varied from 6.0 to 0.5 cm in 0.5-cm fractions until the

corneal touch threshold was found. Each filament length was tested four times. The response was considered negative when no blink was elicited by monofilament touch. A positive response was considered when the animal blinked in equal or more than 50% of the times tested. If blink response could not be elicited at a monofilament length of 0.5 cm, corneal sensitivity was recorded as 0. Following injury, sensitivity was measured every 3 days for 2 weeks and then weekly from 3 to 15 weeks following injury.

Measurement of Tear Volume (Schirmer's Test)

Tear volume was assessed in nonanesthetized mice as previously described^{23,33} with a phenol red-soaked cotton thread (Menicon America, San Mateo, CA, USA) applied using forceps in the lateral canthus for 15 seconds. The wetting length of the thread was read by the examiner under a microscope.

Immunofluorescence Staining and Imaging

From day 1 to day 5 and then at 1, 2, 3, 4, 6, 8, 10, 12, and 15 weeks following injury, 8 mice per time point were euthanized and the eyes enucleated and fixed with Zamboni's fixative (American MasterTech Scientific, Lodi, CA, USA) for 1 hour, followed by three washes with PBS. Then, the corneas were carefully excised along the sclerocorneal rim and double labeled with primary monoclonal rabbit anti-PGP9.5 (1:500) plus rat anti-SP (1:100) antibody or rabbit anti-TRPM8 (1:500) plus rat anti-SP (1:100) antibody in PBS containing 5% goat serum + 0.5% Triton X-100 for 24 hours at room temperature under constant shaking. After washing with PBS (3 × 10 minutes), the corneas were incubated with the corresponding secondary antibodies Alexa fluor 488 goat anti-rabbit IgG (H+L) plus Alexa fluor 594 goat anti-rat IgG (H+L) overnight at 4°C and then washed thoroughly with 1× PBS. Images were taken as described previously.^{22,23,34} Briefly, four radial cuts were performed on each cornea, and the tissue was flatly mounted on a slide with the endothelium side up. Images were acquired with an Olympus IX71 fluorescent microscope. The images at the same layer recorded at the superficial or subbasal layer were merged together to build an entire view of the corneal epithelial nerves.

Retrograde Tracing

Retrograde tracing was used to explore the origin of SP and TRPM8 of sensory neurons in the TG that innervate the corneal epithelium. Five adult normal mice were anesthetized as previously described, and the central cornea was injured by rotating a 1.5-mm-diameter sterile trephine on the corneal surface. Then, a piece of circular filter paper soaked in the retrograde tracer Fast Blue (FB) (5% in distilled water) was placed directly onto the circled cornea for 15 minutes and then extensively washed with PBS. After 1 week, the animals were killed by cervical dislocation and the TG were immediately removed and fixed in Zamboni's fixative for 2 hours in the dark. After washing thoroughly with PBS, the whole TG were embedded in optimal cutting temperature (OCT) compound and serial 10-µm cryostat sections were cut, dried at room temperature for 2 hours and stored at -20°C in dark until use. For immunofluorescence, the sections were double labeled with rabbit anti-TRPM8 (1:500) plus rat anti-SP (1:100) antibodies and followed by correspondent secondary antibodies, as described above. To calculate the relative content of TRPM8 and SP in corneal afferent TG neurons, 12 sections were randomly selected from 4 mice and counted in a blind fashion. In the same image, the FB-labeled neurons were used

to represent the total number of corneal afferent TG neurons. The relative content was expressed as the ratio of TRPM8- or SP-positive neurons and FB-labeled neurons.

TG Gene Expression Analysis

To investigate the TG gene expression after corneal injury, ipsilateral ganglia were harvested at different times after corneal wound and kept in RNAlater solution (Ambion, Austin, TX, USA) for storage without jeopardizing RNA quality or quantity. TG from noninjured mice were used as the control. TG samples were homogenized on ice with a Dounce homogenizer, and total mRNA was extracted using an RNeasy mini kit (Qiagen, Inc., Germantown, MD, USA) as described by the manufacturer. Purity and concentration of RNA were determined with a NanoDrop ND-1000 spectrophotometer (Thermo Fisher Scientific, Waltham, MA, USA). RNA samples were stored at -80°C until they were used. For quantitative PCR, the Biomark HD system (Fluidigm, San Francisco, CA, USA) was used as previously described.³³ Briefly, 200 ng of mRNA was reverse-transcribed using iScript Reverse Transcription Supermix (Bio-Rad, Hercules, CA, USA) and then the cDNA was preamplified using the PreAmp Master Mix (PN 100-5580; Fluidigm) and pool delta gene assays of 96 primer pairs.^{33,35} Next, the preamplified products were treated with Exonuclease I (New England Biolabs, Ipswich, MA, USA) and subjected to 96.96 Dynamic Array IFC for Gene Expression (BMK-M-96.96; Fluidigm) according to the manufacturer's guidance. Data were collected and analyzed using Fluidigm real-time PCR analysis software. The gene expression data were normalized to noncorneal injury samples using the $\Delta\Delta C_t$ method.

Data Analysis

Nerve fiber densities within the central area (about 3.14 mm^2 per cornea) were assessed as a percentage of whole-mount images. To get a better contrast, the fluorescent images were changed to grayscale mode and placed against a white background using Photoshop imaging software (Adobe Systems, Inc., San Jose, CA, USA). The subbasal nerve fibers in each image were carefully drawn with 4-pixel lines following the course of each fiber by using the brush tool in Photoshop (Adobe) imaging software. The nerve area and the total area of the image were obtained by using the histogram tool. The percentage of total nerve area was quantified for each image as described previously.^{22,23} Nerve terminals in superficial epithelia within the central zone were calculated by directly counting the number of terminals in each image recorded with a $20\times$ objective lens. The terminal numbers in each image were directly counted by using ImageJ software (version 1.50i; National Institutes of Health, Bethesda, MD, USA). Because each image took up an area of 0.15 mm^2 , the terminal numbers per mm^2 were calculated. Data were expressed as means \pm SD. Statistical significance ($P < 0.05$) was determined by *t*-test compared with noninjured corneas.

RESULTS

Mapping TRPM8-Positive Epithelial Nerves and Determining Its Relative Content

To map the entire distribution of TRPM8-positive nerves in normal corneal epithelium, 10 corneas were labeled with monoclonal rabbit anti-TRPM8 antibody. Figure 1A shows representative images recorded from two eyes of the same mouse. The images were acquired with a $10\times$ objective lens and reconstructed by merging both terminals and subbasal

nerves together. For better contrast, the color for terminals was changed to pink. TRPM8-positive subbasal nerve fibers run from the periphery and converge into the central area to form the whirl-like structure or vortex (Fig. 1B). Along the path of nerve fibers, fine terminals were budded to innervate the epithelium.

To study the distribution of TRPM8- and SP-positive nerve fibers in the corneal epithelium, 10 corneas were double labeled with rat monoclonal anti-SP plus rabbit monoclonal anti-TRPM8 primary antibodies or plus rabbit monoclonal anti-PGP9.5 as a pan marker for total corneal nerves. Figure 1C shows representative images recorded from two eyes of the same mouse, in which the right eye (OD) was double labeled with SP+PGP9.5, while the left eye (OS) was labeled with SP+TRPM8. All SP-positive nerve fibers were labeled with PGP9.5, and a small number of SP-positive nerve fibers and nerve endings were also positively labeled by TRPM8, as shown in more detail in Figure 1D. Morphologically, TRPM8-positive nerve endings appeared to be longer with more divisions than the SP-positive nerve terminals.

To calculate the relative abundance of SP and TRPM8 with respect to the total epithelial nerves, 10 corneas were triple labeled with SP, TRPM8, and PGP9.5 primary antibodies. Considering that TRPM8 and PGP9.5 antibodies are both raised from rabbit, we labeled the corneas in two steps. First, the corneas were incubated with a set of primary antibodies (SP + PGP9.5 together) and corresponding secondary antibodies (Alexa fluor 594 goat anti-rat IgG [H+L] plus Cy5-conjugated goat anti-rabbit IgG [H+L]), as described above. Afterward, the corneas were thoroughly washed with PBS and then incubated with the third primary antibody TRPM8 in PBS containing 5% goat serum + 0.5% Triton X-100 for 24 hours at room temperature followed by the corresponding secondary antibody (Alexa fluor 488 goat anti-rabbit IgG [H+L]). Representative images of subbasal and nerve terminals triple labeled in the vortex area are shown in Figure 2A. Labeled nerves were quantified as described in the Methods.

In the central area of the cornea, SP-positive nerve fibers constituted $57.7\% \pm 7.2\%$ of the total subbasal nerve content, whereas TRPM8-positive nerves were $22.5\% \pm 6.6\%$ ($n = 10$ eyes; $*P < 0.001$) (Fig. 2B). The percentage of SP positive terminals was also higher ($58.8\% \pm 8.6\%$) than the percentage of TRPM8-positive terminals ($26.4\% \pm 6.6\%$, $*P < 0.001$) (Fig. 2C). In addition, a very small number of nerves showed TRPM8 and SP both positive, accounting for $1.15\% \pm 0.5\%$ of total subbasal nerves ($n = 5$ eyes). To investigate the neuronal origin of TRPM8 and SP nerve fibers in the TG, FB-labeled ipsilateral TGs, through retrograde tracing, were double labeled with antibodies for SP and TRPM8 (Fig. 2D). The results clearly show that SP (red) and TRPM8 (green) are expressed in different neurons and that SP-positive neurons ($28.94\% \pm 6.46\%$) are more abundant than TRPM8 positive neurons ($14.75\% \pm 5.63\%$, $n = 4$ TGs, $P < 0.001$).

Repair of Corneal Nerves After Injury

Immediately after injury, immunofluorescence nerves label with PGP9.5 showed that all epithelial nerves, including terminals and subbasal bundles, together with the anterior stromal branches were ablated (Fig. 3A, yellow arrows show the remaining deep stromal branches). Figure 3B showed that corneal stromal nerve regeneration begins at the nerve stump. On the first day after injury, short shoots sprouting from nerve stumps were detected (as indicated by red arrows). In the next few days, the shoots grew longer (yellow arrows), some of which extended within the stroma to reconstruct the stromal neural network, but most of them were upward, producing many branchlets in the epithelial layer where they presented in

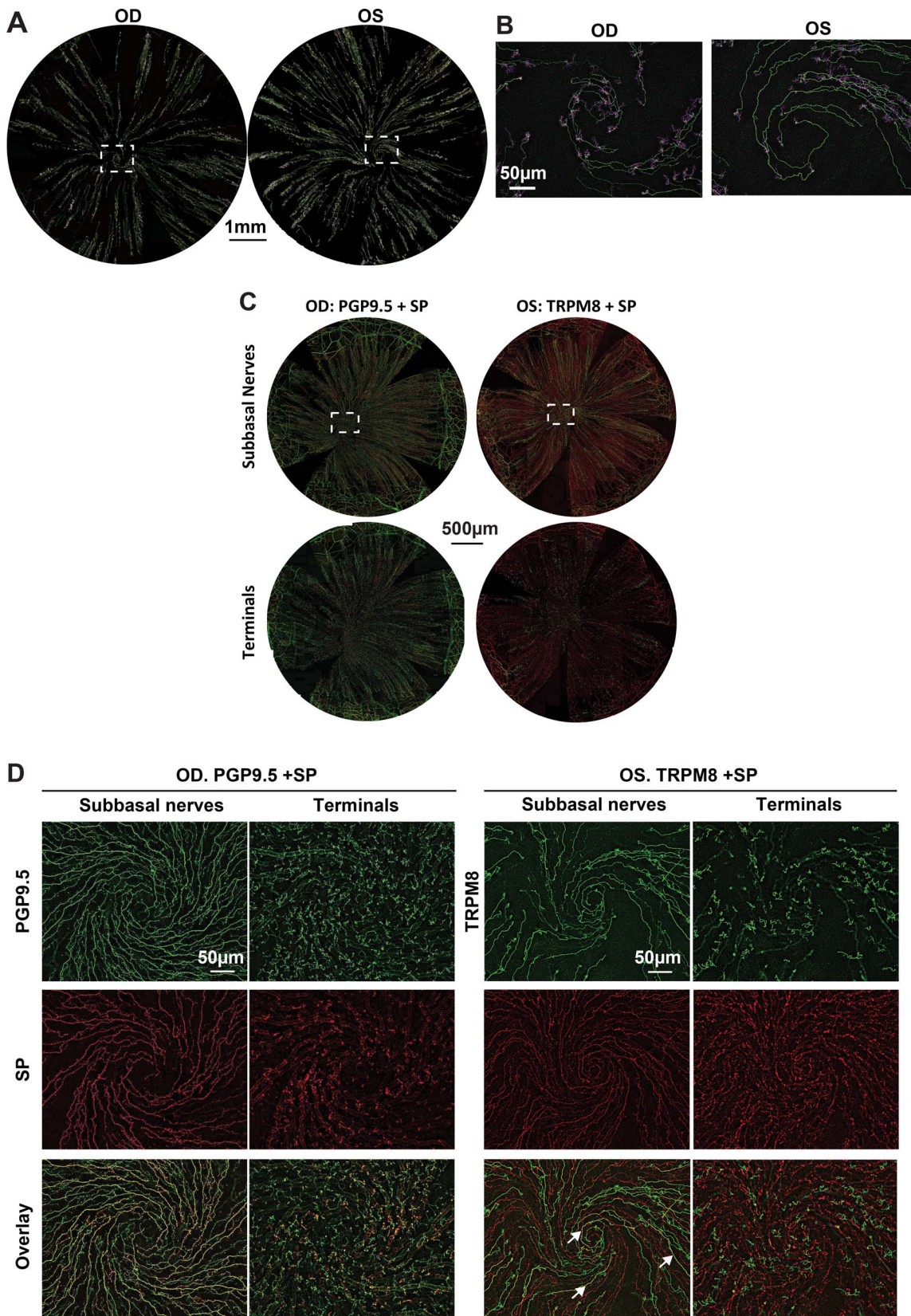


FIGURE 1. Corneal TRPM8 nerve architecture and differences with SP nerves. (A) The whole corneas were labeled with TRPM8 antibody, and images were recorded in a time-lapse mode with a 10× objective lens. The images recorded at the same layer were connected to construct the entire image. Each layer consisted of about 35 images. The reconstructed images were merged with both the superficial terminals and subbasal bundles. For better contrast, the images for terminals were changed to pink color. Images in (B) show the detailed nerve architecture of TRPM8 positive nerves in the vortex. (C) Entire view of corneal subbasal epithelial nerves and superficial terminals. In OD, green is PGP9.5-positive nerves and red corresponds to SP-positive nerves. In OS, green is TRPM8-positive nerves. (D) Highlighted images show the detailed nerve architecture recorded at the superficial nerve terminals and subbasal layers in the vortex. Arrows in the overlay figure show small areas of nerves double stained with SP and TRPM8.

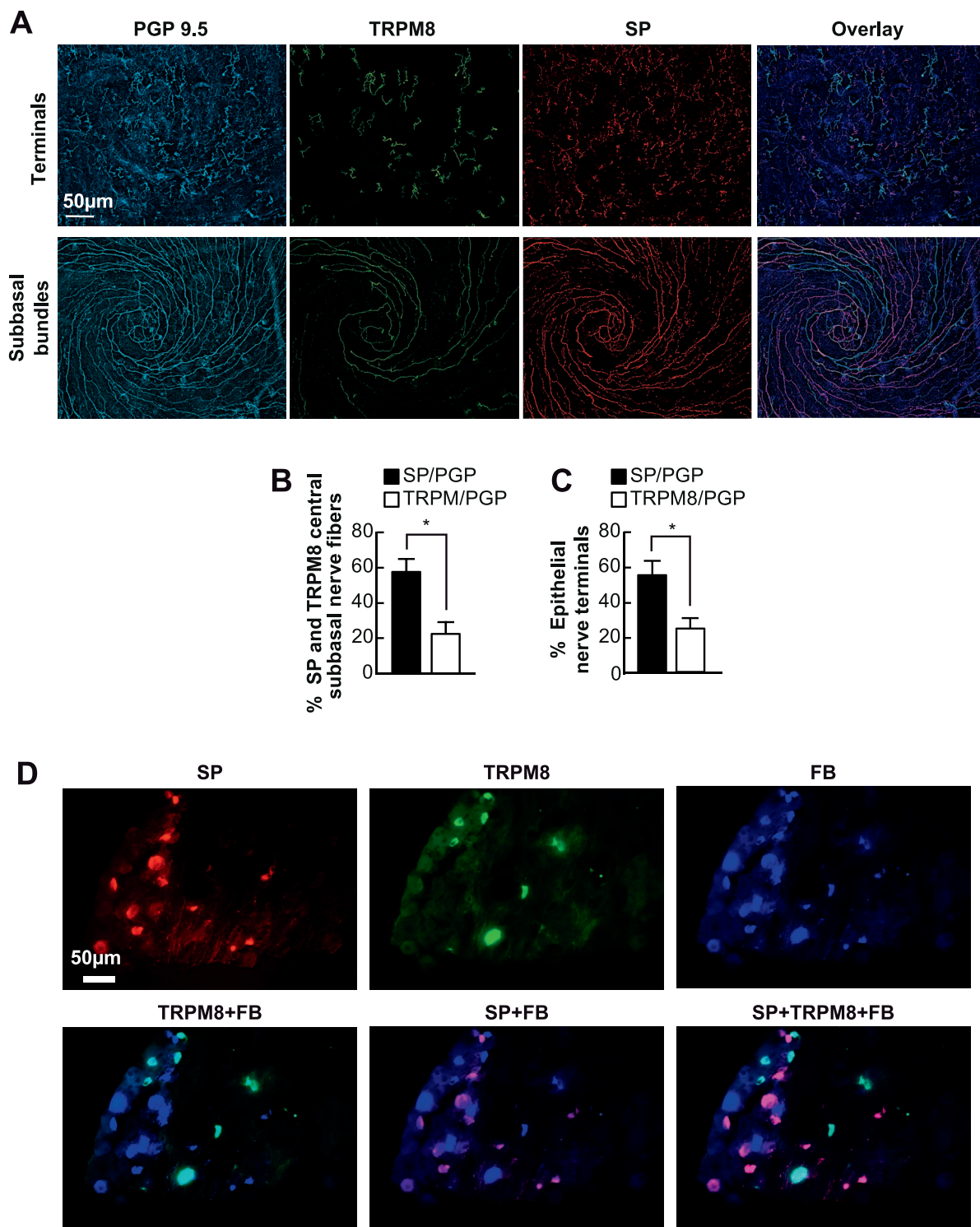


FIGURE 2. Relative content of corneal epithelial TRPM8 and SP nerves. **(A)** Representative images of subbasal and nerve terminals in the vortex area labeled with PGP9.5, SP and TRPM8. **(B, C)** Percentage of TRPM8- and SP-positive subbasal bundles and nerve terminals versus total nerve area (PGP9.5-positive nerves) in each image. A total of 20 images for TRPM8 or SP and the same number of images for PGP9.5 were recorded from 10 corneas. Data expressed as average \pm SD. **(D)** Localization of TRPM8- and SP-positive neurons in TG. Ipsilateral TG were FB-labeled through retrograde tracing. One week later, the whole TGs were processed for immunofluorescence with SP and TRPM8 antibodies. Representative images were recorded with a 20 \times objective lens.

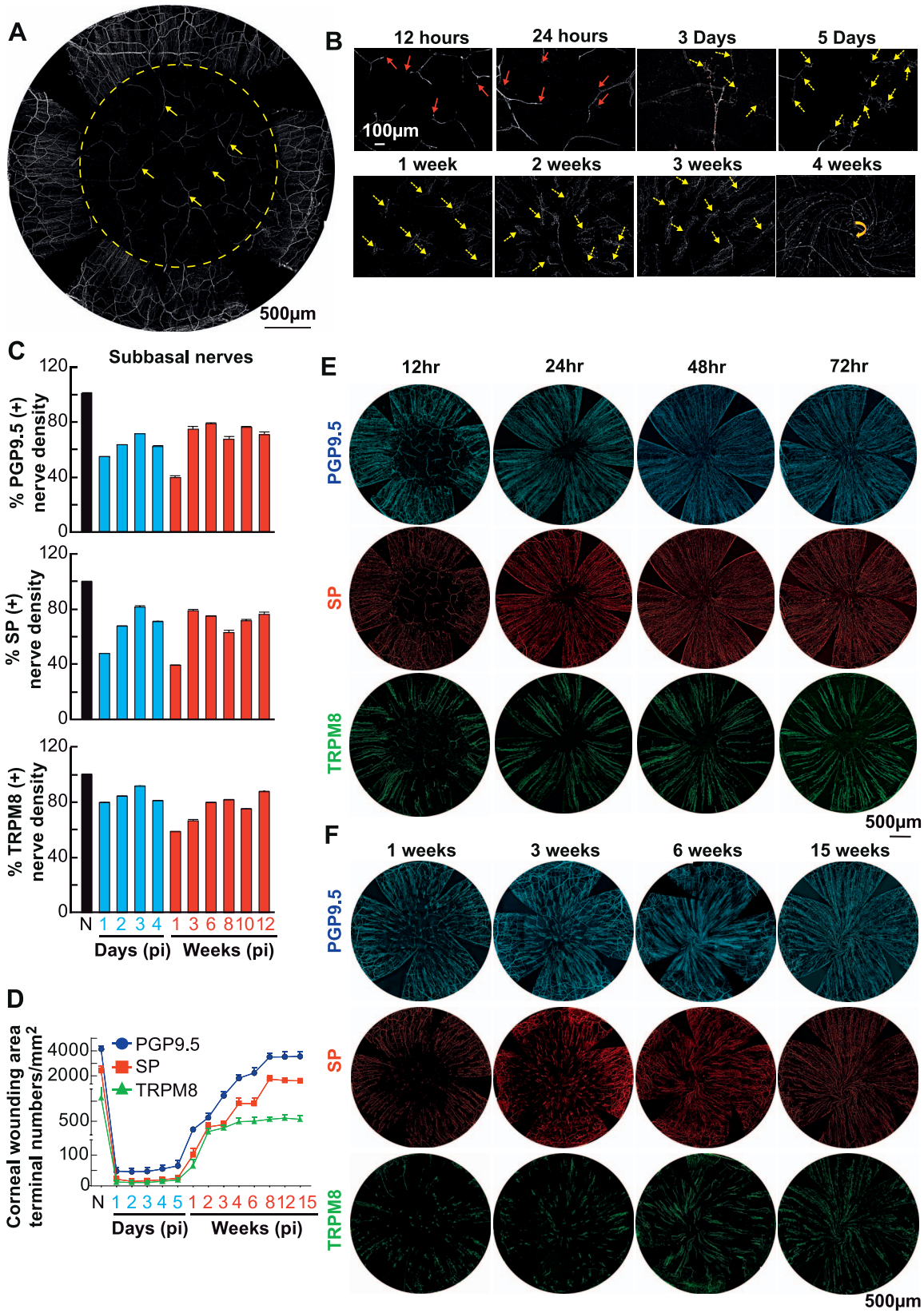


FIGURE 3. Time course of corneal nerve regeneration after injury. (A) Entire view of corneal nerve architecture immediately following the surgery. All epithelial and anterior stromal nerve branches within a total area of about 3.14 mm² ($\Phi = 2$ mm) were removed by using a corneal rust ring remover under an Evolution Zoom Microscope (63122; Seiler Instrument Inc., St. Louis, MO, USA), but deeper stromal nerves still were present. Representative images were labeled with monoclonal rabbit anti-PGP9.5 antibody and recorded at a magnification of 10 \times objective. A total of 35 images were merged together to reconstitute the entire view of corneal nerve architecture. Three representative videos showing the details of corneal nerve regeneration in the central corneas recorded on 1 and 3 days and 3 weeks after injury are provided in the supplementary materials

(Supplementary Video S1, S2, S3). **(B)** Representative images labeled with PGP9.5 antibody and recorded from postoperative 12 hours to 4 weeks showing the nerve regeneration. *Red arrows* indicate the newly regenerated nerve buds. *Yellow arrows* indicate the new epithelial nerve bundles originated from the underlying stromal nerve branches. *Yellow arrow* at 4 weeks indicates the vortex running clockwise. **(C)** Central subepithelial PGP9.5-, SP-, and TRPM8-labeled nerve density at different time postinjury (pi). Data at each time point represent the average percentage of subepithelial nerve density postinjury versus preinjury (N). At each time point, 8 mice were euthanized, 4 corneas were double labeled with PGP + SP, and 4 corneas were double labeled with TRPM8 + SP. All the time points are significantly decreased respect to noninjury values ($P < 0.05$). **(D)** Changes in the number of PGP9.5, SP and TRPM8 nerve terminals pi. Significant difference at 8 to 15 weeks compared to noninjured ($P < 0.001$). Representative images showing the epithelial terminals at 1, 3, 5, and 7 days and at 3, 6, 8, and 12 weeks are provided in Supplementary Figure S1 (recorded at a magnification of 10 \times objective). **E** and **F** are representative images showing the entire subbasal nerves labeled with PGP9.5, SP, and TRPM8 antibodies at early (12–72 hours) and late (1–15 weeks) stages. At each time point, a total of 16 images recorded from the central cornea of 4 mice were calculated for each antibody. Data are expressed as average \pm SD.

clusters. During the first few days up to 1 week, the nerve fibers in the epithelia grew without a given direction, but from 1 week on, they grew centripetally. Four weeks after injury, the epithelial nerves formed a whirl-like structure in the central zone (yellow arrow).

We followed the regeneration of total, SP- and TRPM8-labeled nerves up to 15 weeks. Epithelial nerve regeneration was divided into two distinct phases. First, regenerated epithelial nerves originated from the remaining epithelial nerve bundle around the wound, which extended centripetally to innervate the injured area. By day 3, the density of total subbasal nerve fibers in the wound area reached about 70% of normal levels (Figs. 3C, 3D). The densities of SP- and TRPM8-positive nerve fibers recovered 82% and 92% of the normal levels respectively. Second, from days 4 to 7, the total and positive SP nerve density decreased, and at 1 week after injury they represent 39% of normal levels, whereas TRPM8-positive

nerves are 58% of the noninjured corneas (Figs. 3C, 3F). One week after the wound, the regenerated epithelial nerves were mainly derived from the new branches of the stromal nerves, as shown in Figure 3B. With the growth of new regenerated epithelial bundles, total nerve density and SP- and TRPM8-positive nerve fibers gradually increased. However, by 15 weeks postsurgery, corneal innervation still was not fully restored (Figs. 3C, 3F).

In the first 5 days after the injury, the numbers of total epithelial nerve endings labeled with PGP9.5, SP, and TRPM8, were constantly low (Fig. 3D). At day 5, the average number of nerve endings per square millimeter was 65 ± 29 for PGP 9.5 (mean \pm SD), 25 ± 10 for SP, and 19 ± 7 for TRPM8. By day 7, after the wound with the growth of epithelial nerves derived from the underlying stromal nerve branches, the total number of terminals begin to increase. TRPM8 nerve terminals plateaued at 4 weeks, whereas SP- and PGP9.5-positive

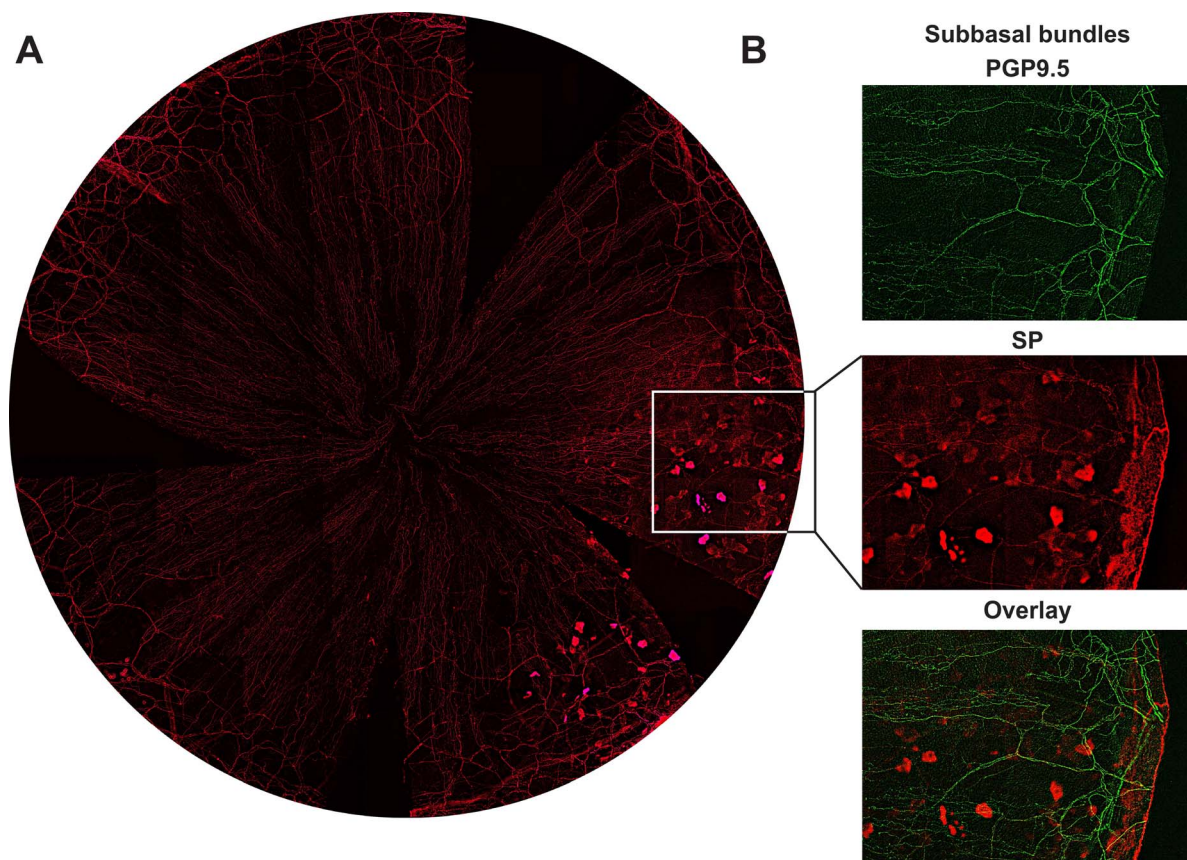


FIGURE 4. Abnormal expression of SP neuropeptide after corneal injury. **(A)** Representative image shows corneal epithelial SP positive nerves and epithelial cells recorded from a mouse cornea at 8 weeks after injury. **(B)** Highlighted images as framed in **(A)** show the detailed structures of subbasal bundles and epithelial cells double stained with PGP9.5 and SP.

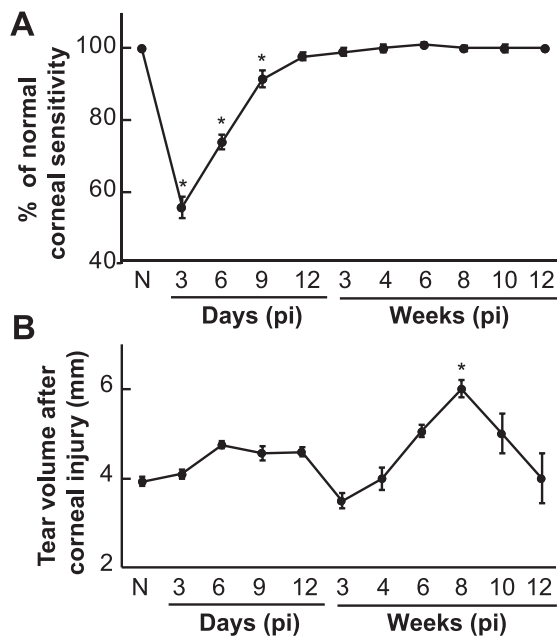


FIGURE 5. Changes in corneal sensitivity and tear production pi. (A) Data at each time point represent the average percentage \pm SD of corneal sensitivity postinjury versus preinjury (N). At least 8 corneas (8 mice) were measured. (B) Tear volume data at each time point are the average \pm SE of at least 8 eyes (8 mice).

terminals continued to increase and plateau at 8 weeks once the total nerve density reached 85% and SP-positive nerve terminals reach 68% of their normal values ($P < 0.001$). After 15 weeks of corneal injury, the number of TRPM8-positive terminals was only 53% of the normal values ($P < 0.001$).

It is worth noting that from 6 weeks to the end of the experiment (15 weeks) after injury between, 12% to 25% of the corneas have quadrant epithelial lesions (Fig. 4A). Epithelial cells in the lesion area were strongly expressing SP, whereas SP-positive epithelial nerve fibers and terminals in that area were significantly reduced (Fig. 4B).

Corneal Sensitivity and Tear Production After Injury

One day before surgery, corneal sensitivity was measured in all eyes using a Cochet-Bonnet esthesiometer with an average of 5.5 ± 0.5 cm (mean \pm SD, $n = 60$ eyes), which was used as baseline values (N). Postinjury measurements began on the third day after surgery when the epithelial wound was completely closed. In the first 2 weeks, the measurements were taken every 3 days and, afterward, every 1 or 2 weeks. As shown in Figure 5A, the corneal sensitivity on day 3 decreased to 50% of the normal level and then gradually increased, reaching normal levels at 12 days.

Tear production was measured according to the same schedule as corneal sensitivity, but the interval between the measurements of sensitivity and tear production was 6 hours. As shown in Figure 5B, the tear volume before surgery (N) was 4 ± 0.2 mm (mean \pm SE, $n = 60$ eyes). Six days after injury, the volume of tears increased and remained constant until day 12. From the second to the third week after the wound, the volume of tears was significantly reduced and then, gradually increased, reaching its highest value at week 8 with 5 ± 0.4 mm ($n = 15$ eyes). After that, tear production gradually decreased and returned to normal levels at week 15.

TG Gene Expression Following Corneal Injury

The Fluidigm integrated fluidic circuits 96 genes \times 96 samples platform was used to analyze gene expression in the TG after corneal injury. All genes with more than two-fold changes, in comparison to TG from noninjured mice, were considered significant. The heatmap (Fig. 6) indicated two clusters of gene profile in the TG at many time points of this analysis: (1) downregulated genes (blue color) from 1 hour until 96 hours or 1 week and (2) upregulated genes (red color) from the beginning of the injury. As shown in Figure 6, several other wound healing- or nerve regeneration-related genes, including nuclear factor 2 (*nrf2*), brain-derived neurotrophic factor (*bdnf*), calbindin 1 (*calb1*), caspase 1 (*casp1*), and sequestosome 1 (*sqstm1*), were downregulated with the lowest expression observed at 96 hours or 1 week after injury. The expression of *bdnf* was inhibited longer, up to 3 weeks after injury. The hypoxia inducible factor 1 α (*bif1a*) gene was inhibited at 1 hour after the injury, and this inhibition decreased over time until 1 week. Three autophagosome-related genes, *atg3*, *atg5*, and *atg10* were also inhibited during the first 96 hours to 1 week after injury. There was a significant activation of survival genes, such as bcl-2-like protein 10 (*bcl2l10*) and baculoviral inhibitor of apoptosis protein (IAP) repeat containing 3 (*birc3*), as well as proresolution genes arachidonate 15-lipoxygenase (*alox15*) and peroxisome proliferator-activated receptor α (*ppar- α*). This activation was observed from 1 hour to 2 weeks after corneal injury.

We also investigated the gene expression of SP and TRPM8 in the TGs. Expression of *trpm8* fluctuated after injury, but the changes were not significant at any time (Fig. 6). On the other hand, the *tac1* gene encoding the SP neuropeptide was significantly downregulated at most time points after injury.

DISCUSSION

Chronic neuropathic pain arising from peripheral nerve damage is a severe clinical problem with limited treatment options. During corneal refractive surgery, damage to the nociceptors can cause DELP.²⁻¹³ Changes in corneal nerve structure and sensory responses after surgery are thought to play a key role in the etiology, but the exact pathogenesis remains unclear. A recent study has reported that PRK results in both functional and morphologic alterations in mechanical, polymodal, and cold sensory nerve fibers of the cornea.¹⁸

We found that epithelial nerve regeneration has two origins. At an early stage (1-3 days), the epithelial nerves in the wound area come from the remaining bundles around the wound, which extend radially to the center along with the sliding epithelium. Therefore, in the first few days, epithelial nerve density increased rapidly, reaching about 70% of normal levels by day 3. Surprisingly, from day 4 to day 7, when the epithelial wound was already closed, the epithelial nerve density gradually decreased. By day 7, the epithelial nerves were reduced to 39% of normal levels. Many factors may contribute to the regeneration and degradation of nerve fibers, but based on previous studies, one mechanism may involve the expression of fibronectin³⁶ and matrix metalloproteinases (MMPs) during wound healing.³⁷⁻³⁹ Fibronectin (FN) has been shown to support neurites and axonal outgrowth.⁴⁰⁻⁴² Shortly after wounding, there is a layer of FN and fibrin deposited on the denuded corneal surface, which serve as a temporary basement membrane to facilitate cell migration³⁷ and possible the axonal growth that we observed in the early times after injury. MMPs and their inhibitors regulate extracellular matrix degradation and deposition that are essential for wound reepithelialization.³⁸⁻⁴⁰ Once the wound is closed, the

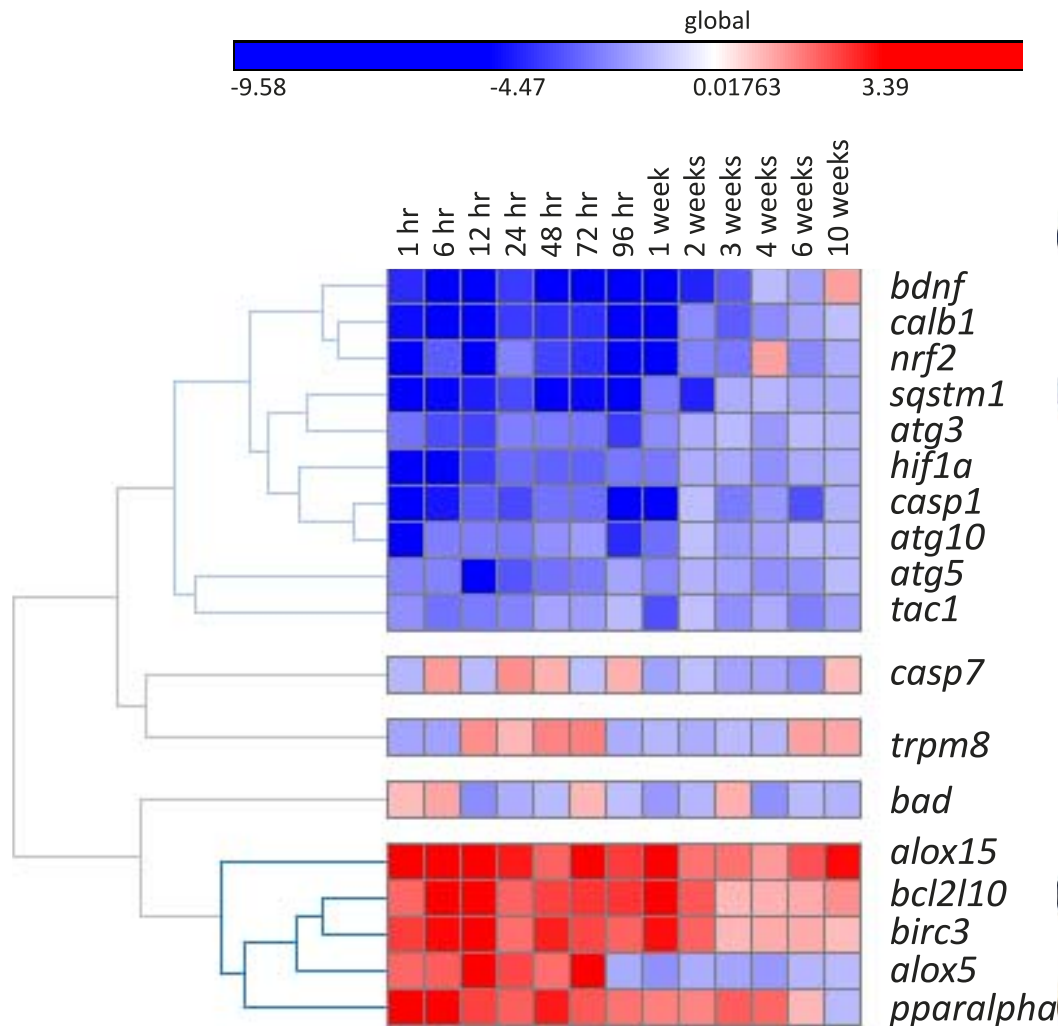


FIGURE 6. TG gene expression following corneal injury. Ipsilateral TG were collected at different times after corneal injury. The values correspond to 3 TG/time and were calculated in comparison to 3 TG of different mouse without injury obtained at the same times that the experimental ones. The Fluidigm integrated fluidic circuits 96 genes \times 96 samples platform was used to analyze TG gene expression. The heatmap indicated two clusters of gene profile in the TG at the time points of this analysis: (1) downregulated genes (*blue colors*) from 1 hour until 96 hour or 1 week and (2) upregulated genes (*red colors*) from the beginning of the injury. All genes with more than two-fold changes, in comparison to the baseline (no injury), were considered significant.

subepithelial FN is degraded by MMPs secreted by the epithelial cells, and therefore the decrease in corneal nerve fibers that we observed from day 4 after injury are consistent with the time of activation of MMPs and degradation of FN. One week after the injury, the epithelial nerves in the wound area are mainly derived from the underlying regenerated stromal nerve branches. Although obvious corneal stromal nerve regeneration was observed at 1 to 3 days after the injury, these nerves did not appear in the epithelial layer until 5 days postwound when the existing epithelial nerves have already been degraded, as discussed above. From 1 week on, the density of epithelial nerves increased over time. However, at 15 weeks after injury, the nerve density did not reach the noninjured level.

Consistent with our recent studies,²² SP nerve fibers in normal mouse corneal epithelium account for approximately 58% of total subbasal nerves. After injury, the density of SP nerve fibers in the corneal epithelium have similar changes to that of total epithelial nerves, and at 15 weeks, SP nerve fibers including superficial terminals and subbasal bundles do not recover to normal levels.

Changes in SP expression have been associated with neurogenic inflammation and neuropathic pain.^{20,43} Local injection of SP into the hind paw of rats produces hyperalgesia, allodynia, and an increase in the pain-enhancing action of glutamate.⁴⁴ Our previous study in a mouse diabetes model has shown that diabetes not only reduces corneal epithelial density but also reduces SP nerve fiber content, leading to decreased corneal sensitivity and delayed wound healing.²⁵ Between 12% to 25% of injured eyes developed quadrant epithelial lesions after the wound. SP-positive subbasal nerve fibers and terminals decreased, and conversely, some epithelial cells were strongly stained positive by SP. This is similar to our previous report showing that there was SP-positive staining in the epithelial cells of rabbit cornea after injury.³² Another possibility is that the SP-positive cells are goblet cells. They had been described in the mouse as clusters of cells that increase in number after corneal wounds.⁴⁵ Abnormal expression of SP may lead to postoperative neurogenic inflammation and neuropathic pain.

Our results show that in the central epithelium of normal adult mice, TRPM8-positive nerves account for $22.5\% \pm 6.5\%$

of the total subbasal bundles and for $26.3\% \pm 6.4\%$ of the total superficial endings. These proportions are similar to a recent report in a transgenic TRPM8 mouse fluorescent with YFP.¹⁹ Consistent with previous studies, we found that corneal epithelial TRPM8 and SP nerve fibers have different neuronal origins and that SP-positive neurons are more abundant than TRPM8 neurons. The TRPM8 nerve endings appear longer and more branched, in agreement with a recent study in guinea pig corneas,⁴⁶ suggesting that this morphology will increase the number of cold receptors in the corneal epithelium. Interestingly, a number of TRPM8+ terminals also contain SP. These may correspond to a subpopulation of high-threshold, low-background, cold-sensitive fibers associated with nociceptive central neurons that can be related to unpleasant dry sensations.¹⁵

Postinjury changes in TRPM8 content in the subbasal nerves were similar to SP. However, from 3 to 12 weeks after injury, TRPM8 nerve endings did not change significantly with increasing epithelial nerve density from 3 weeks to 12 weeks after injury and were still only about half of the normal level.

Hypersensitivity to cold temperature, manifested clinically as cold hyperalgesia or cold allodynia, is a frequent symptom of patients with refractive surgery-induced DELP. In chronic pain states, the central sensitization that consolidates hypersensitive pain behavior is weakened by the TRPM8-positive input, acting to gate-out nociceptive processing and producing an analgesic effect.²⁸ Therefore, our results suggest that the insufficient recovery of corneal TRPM8 nerve terminals following corneal injury may contribute to postsurgery DELP.

Nerve terminals are responsible for transducing sensory stimuli into nerve signals, and their numbers are directly proportional to corneal sensitivity.¹⁷ Our results showed that although the number of superficial nerve endings was much lower than normal in the first 2 months after injury, corneal sensitivity still recovered fast, especially from day 3 to day 12. At 2 weeks after injury, when the corneal sensitivity has reached normal levels, the number of nerve terminals are only 15% of the noninjured corneas. One possibility is that the Cochet-Bonnet esthesiometer only detects mechanoreceptors and no chemo- and thermoreceptor activity. Another possible explanation is that newly regenerated corneal nerves are hypersensitive after injury.

Tear production is often used as an indicator of neurologic recovery after corneal refractive surgery. Patients undergoing refractive surgery often complain of dry eye symptoms, but when their tear production is measured it is found that the tear volume is normal. It is now well known that this phenomenon is typical of DELP.^{14-16,47,48} We found there is an unstable tear production after surgery, and except for the third week after injury, the number of tears increase and was highest at week 8. The increase in tears in the early postoperative period may be related to wound response caused by surgery; and excessive secretion of tears in the late stage of injury may reflect corneal nerve hypersensitivity. In the latter case, although the density of corneal epithelial nerve fibers is low due to the high sensitivity of the nerves, any external stimulation to the ocular surface may cause tearing.

We also examine the effect of corneal surgery on the TG expression of selective genes associated with corneal wound healing, inflammation, apoptosis, and nerve regeneration. Of the genes whose expression was significantly decreased, hypoxia-inducible factor 1 α (HIF1 α). Studies have reported that knockdown of HIF-1 α in vitro or conditional knock out in vivo impairs sensory axon regeneration.⁴⁹ Other genes downregulated were *nrf2*, *bdnf*, *calb1*, *casp1*, and *sqstm1*. An in vivo study has shown that corneal epithelial cell migration and wound healing were significantly delayed in *nrf2* knockout mice.⁵⁰ The expression of *bdnf* in the TG was

inhibited up to 3 weeks after injury. Recent studies from our lab have shown that there is an increase in gene expression of this neurotrophin in mouse corneas after 3-hour injury and stimulation of nerve regeneration with pigment epithelium-derived factor (PEDF) + docosahexaenoic acid (DHA), and this increase is followed by the secretion of BDNF in tears at 6 hours.³⁵

An interesting finding is the decreased expression of the autophagosome-related genes *atg3*, *atg5*, and *atg10*. Autophagy has been demonstrated as an axonal regeneration factor in the dorsal root ganglia.^{51,52} The upregulation of autophagy, especially in the Wallerian degeneration (WD), is regarded as a key component to enhance the axonal regeneration.⁵³ In the cornea, however, the stage of regeneration is completely different. As shown in Figure 3C, WD does not occur immediately after corneal nerve injury because corneal nerves grow faster in the first few days after injury with a peak of corneal nerve density at 72 hours after injury. This suggests that the WD process occurred at later time point when the corneal nerve density was degenerated to establish the functional axonal network in the cornea. For this reason, our data indicate that autophagy is not an important factor in corneal nerve regeneration, and therefore, the expression of autophagosome-related genes decreased at the beginning of the regeneration process.

On the other hand, there was a significant activation of survival genes *bcl2110* and *birc3* as well as the proresolution genes *alox15* and *ppar- α* . The cell membrane phospholipids phosphatidylcholine and phosphatidylethanolamine of the TG are enriched in DHA.³⁵ The *alox15* gene codifies 15-lip-oxygenase, a key enzyme in the synthesis of DHA-derived mediators such as NPD1, which, in turn, activate the cellular survival machinery, including *birc3* and *bcl2110* gene expression.⁵⁴ This effect ensures the homeostasis of the TGs from the axonal removal in the cornea as well as maintains the microsystem of the regenerating progression. Finally, the unstable expression of *trpm8* and downregulation of *tac1* may explain the lower densities of TRPM8- and SP-positive axons and terminals in the cornea after injury.

In summary, we used our improved technique of immunofluorescence and imaging to provide, for the first time, a complete map of entire epithelial TRPM8 nerve architecture and the relative content in mouse cornea. We have also investigated the remodeling course of corneal nerves and TG gene expression following corneal experimental surgery. The persistence of a regenerating phenotype of corneal nerves long after wound closure, abnormal SP expression, and low amounts of TRPM8 terminals and changes in gene expression in TG may contribute to the pathogenesis of DELP.

Acknowledgments

Supported by the National Eye Institute Grant R01 EY19465.

Disclosure: **J. He**, None; **T.L. Pham**, None; **A.H. Kakazu**, None; **H.E.P. Bazan**, None

References

- Rózsa AJ, Beuerman RW. Density and organization of free nerve endings in the corneal epithelium of the rabbit. *PAIN*. 1982;14:105-120.
- Rosenthal P, Borsook D. Ocular neuropathic pain. *Br J Ophthalmol*. 2016;100:128-134.
- Raof D, Pineda R. Dry eye after laser in-situ keratomileusis. *Semin Ophthalmol*. 2014;29:358-362.
- Solomon KD, Holzer MP, Sandoval HP, et al. Refractive surgery survey 2001. *J Cataract Refract Surg*. 2002;28:346-355.

5. Levitt AE, Galor A, Weiss JS, et al. Chronic dry eye symptoms after LASIK: parallels and lessons to be learned from other persistent post-operative pain disorders. *Mol Pain*. 2015;11:21.
6. Shtein RM. Post-LASIK dry eye. *Expert Review Ophthalmol*. 2011;6:575-582.
7. Tuisku IS, Lindbohm N, Wilson SE, Tervo TM. Dry eye and corneal sensitivity after high myopic LASIK. *J Refract Surg*. 2007;23:338-342.
8. Hovanesian JA, Shah SS, Maloney RK. Symptoms of dry eye and recurrent erosion syndrome after refractive surgery. *J Cataract Refract Surg*. 2001;27:577-584.
9. Murakami Y, Manche EE. Prospective, randomized comparison of self-reported postoperative dry eye and visual fluctuation in LASIK and photorefractive keratectomy. *Ophthalmology*. 2012;119:2220-2224.
10. Nettune GR, Pflugfelder SC. Post-LASIK tear dysfunction and dysesthesia. *Ocul Surf*. 2010;8:135-145.
11. Denoyer A, Landman E, Trinh L, Faure JF, Auclin F, Baudouin C. Dry eye disease after refractive surgery: comparative outcomes of small incision lenticule extraction versus LASIK. *Ophthalmology*. 2015;122:669-676.
12. Bower KS, Sia RK, Ryan DS, Mines MJ, Dartt DA. Chronic dry eye in PRK and LASIK: manifestations, incidence and predictive factors. *J Cataract Refract Surg*. 2015;41:2624-2634.
13. Cohen E, Spierer O. Dry eye post-laser-assisted in situ keratomileusis: major review and latest updates. *J Ophthalmol*. 2018;2018:4903831.
14. Nichols KK, Nichols JJ, Mitchell GL. The lack of association between signs and symptoms in patients with dry eye disease. *Cornea*. 2004;23:762-770.
15. Belmonte C. Eye dryness sensations after refractive surgery: impaired tear secretion or phantom cornea. *J Refract Surg*. 2007;23:598-602.
16. Rosenthal P, Baran I, Jacobs DS. Corneal pain without stain: is it real? *Ocul Surf*. 2009;7:28-40.
17. Belmonte C, Acosta MC, Gallar J. Neural basis of sensation in intact and injured corneas. *Exp Eye Res*. 2004;78:513-525.
18. Bech F, González-González O, Artme E, et al. Functional and morphologic alterations in mechanical, polymodal, and cold sensory nerve fibers of the cornea following photorefractive keratectomy. *Invest Ophthalmol Vis Sci*. 2018;59:2281-2292.
19. Alcalde I, Inigo-Portugues A, Gonzalez-Gonzalez O, et al. Morphological and functional changes in TRPM8-expressing corneal cold thermoreceptor neurons during aging and their impact on tearing in mice. *J Comp Neurol*. 2018;526:1859-1874.
20. De Felipe, Herrero JF, O'Brien JA, et al. Altered nociception, analgesia and aggression in mice lacking the receptor for substance P. *Nature*. 1998;392:394-397.
21. Motterle L, Diebold Y, Enriquez de Salamanca A, et al. Altered expression of neurotransmitter receptors and neuromediators in vernal keratoconjunctivitis. *Arch Ophthalmol*. 2006;124:462-468.
22. He J, Bazan HEP. Neuroanatomy and neurochemistry of mouse cornea. *Invest Ophthalmol Vis Sci*. 2016;57:664-674.
23. He J, Pham TL, Kakazu AH, Bazan HEP. Recovery of corneal sensitivity and increase in nerve density and wound healing in diabetic mice after PEDF plus DHA treatment. *Diabetes*. 2017;66:2511-2520.
24. Bautista DM, Siemens J, Glazer JM, et al. The menthol receptor TRPM8 is the principal detector of environmental cold. *Nature*. 2007;448:204-208.
25. Quallo T, Vastani N, Horridge E, et al. TRPM8 is a neuronal osmosensor that regulates eye blinking in mice. *Nat Commun*. 2015;6:7150.
26. Parra A, Madrid R, Echevarria D, et al. Ocular surface wetness is regulated by TRPM8-dependent cold thermoreceptors of the cornea. *Nat Med*. 2010;16:1396-1399.
27. Proudfoot CJ, Garry EM, Cottrell DF, et al. Analgesia mediated by the TRPM8 cold receptor in chronic neuropathic pain. *Curr Biol*. 2006;16:1591-1605.
28. Liu B, Lu F, Balakrishna S, Sui A, Morris JB, Jordt SE. TRPM8 is the principal mediator of menthol-induced analgesia of acute and inflammatory pain. *PAIN*. 2013;154:2169-2177.
29. Fernández-Peña C, Viana F. Targeting TRPM8 for pain relief. *Open Pain J*. 2013;6:154-164.
30. Belmonte C, Gallar JG. Cold thermoreceptors, unexpected players in tear production and ocular dryness sensations. *Invest Ophthalmol Vis Sci*. 2011;52:3888-3892.
31. Corcoran P, Hollander DA, Ousler GW III, et al. Dynamic sensitivity of corneal TRPM8 receptors to menthol instillation in dry eye versus normal subjects. *J Ocular Pharmacol Ther*. 2017;33:686-692.
32. Cortina MS, He J, Li N, Bazan NG, Bazan HEP. Recovery of corneal sensitivity, CGRP positive nerves and increased wound healing are induced by PEDF plus DHA after experimental surgery. *JAMA Ophthalmol*. 2012;130:76-83.
33. Pham TL, Kakazu A, He J, Bazan HEP. Mouse strains and sexual divergence in corneal innervation and nerve regeneration. *FASEB J*. 2019;33:4598-4609.
34. He J, Bazan NG, Bazan HEP. Mapping the entire human corneal nerve architecture. *Exp Eye Res*. 2010;91:513-523.
35. Pham TL, He J, Kakazu AH, Jun B, Bazan NG, Bazan HEP. Defining a mechanistic link between pigment epithelium-derived factor, docosahexaenoic acid and corneal nerve regeneration. *J Biol Chem*. 2017;292:18486-18499.
36. Nishida T, Nakagawa S, Nishibayashi C, et al. Fibronectin enhancement of corneal epithelial wound healing of rabbits in vivo. *Arch Ophthalmol*. 1984;102:455-456.
37. Azar DT, Hahn TW, Jain S, Yeh YC, Stetler-Stevenson WG. Matrix metalloproteinases are expressed during wound healing after excimer laser keratectomy. *Cornea*. 1996;15:18-24.
38. Rohani MG, Parks WC. Matrix remodeling by MMPs during wound repair. *Matrix Biol*. 2015;44-46:113-121.
39. Caley MP, Martins VLC, O'Toole EA. Metalloproteinases and wound healing. *Adv Wound Care*. 2015;4:225-234.
40. Lefcort F, Venstrom K, McDonald JA, Reichardt LF. Regulation of expression of fibronectin and its receptor, alpha 5 beta 1, during development and regeneration of peripheral nerve. *Development*. 1992;116:767-782.
41. Tonge DA, Burgh HTD, Docherty R, Humphries MJ, Craig SE, Pizzey J. Fibronectin supports neurite outgrowth and axonal regeneration of adult brain neurons in vitro. *Brain Res*. 2012;1453:8-16.
42. Tom VJ, Doller CM, Malouf AT, Silver J. Astrocyte-associated fibronectin is critical for axonal regeneration in adult white matter. *J Neurosci*. 2004;24:9282-9290.
43. Zubrzycka M, Janecka A. Substance P: transmitter of nociception (Minireview). *Endocr Regul*. 2000;34:195-201.
44. Sahbaie P, Shi X, Guo TZ, et al. Role of substance P signaling in enhanced nociceptive sensitization and local cytokine production after incision. *Pain*. 2009;145:341-349.
45. Pajoohesh-Ganji A, Pal-Ghosh S, Tadvalkar G, Stepp MA. Corneal goblet cells and their niche: implication for corneal stem cell deficiency. *Stem Cells*. 2012;30:2032-2043.
46. Alamri AS, Wood RJ, Ivanusic JJ, Brock JA. The neurochemistry and morphology of functionally identified corneal polymodal nociceptors and cold thermoreceptors. *PLoS One*. 2018;13:e0195108.
47. Galor A, Zlotcavitch L, Walter CD, et al. Dry eye symptom severity and persistence are associated with symptoms of neuropathic pain. *Br J Ophthalmol*. 2015;99:665-668.

48. Mcmonnies CW. The potential role of neuropathic mechanisms in dry eye syndromes. *J Optom.* 2017;10:5-13.
49. Cho Y, Shin JE, Ewan EE, Oh YM, Pita-Thomas W, Cavalli V. Activating injury-responsive genes with hypoxia enhances axon regeneration through neuronal HIF-1 α . *Neuron.* 2015; 88:720-734.
50. Hayashi R, Himori N, Taguchi K, et al. The role of the Nrf2-mediated defense system in corneal epithelial wound healing. *Free Radic Biol Med.* 2013;6:1333-1342.
51. Hou H, Zhang L, Zhang L, et al. Acute spinal cord injury could cause activation of autophagy in dorsal root ganglia. *Spinal Cord.* 2013;51:679-682.
52. He M, Ding Y, Chu C, Tang J, Xiao Q, Luo ZG. Autophagy induction stabilizes microtubules and promotes axon regeneration after spinal cord injury. *Proc Natl Acad Sci U S A.* 2016;113:11324-11329.
53. Jang SY, Shin YK, Park SY, et al. Autophagic myelin destruction by Schwann cells during Wallerian degeneration and segmental demyelination. *Glia.* 2016;64:730-742.
54. Calandria J, Marcheselli VL, Mukherjee PK, Bazan NG. Selective survival rescue in 15-lipoxygenase-1-deficient retinal pigment epithelial cells by the novel docosahexaenoic acid-derived mediator, neuroprotectin D1. *J Biol Chem.* 2009;284: 17877-17882.